Steady Bell State Generation via Magnon-Photon Coupling

H. Y. Yuan,[1,*] Peng Yan,[2] Shasha Zheng,[3,4,5] Q. Y. He,[3,4,5] Ke Xia,[6] and Man-Hong Yung[7,8,9,†]

[1]Department of Physics, Southern University of Science and Technology, Shenzhen 518055, China
[2]School of Electronic Science and Engineering and State Key Laboratory of Thin Films and Integrated Devices, University of Electronic Science and Technology of China, Chengdu 610054, China
[3]State Key Laboratory for Mesoscopic Physics, School of Physics and Frontiers Science Center for Nano-Optoelectronics, Peking University, Beijing 100871, China
[4]Beijing Academy of Quantum Information Sciences, Haidian District, Beijing 100193, China
[5]Collaborative Innovation Center of Extreme Optics, Shanxi University, Taiyuan, Shanxi 030006, China
[6]Beijing Computational Science Research Center, Beijing 100193, China
[7]Institute for Quantum Science and Engineering and Department of Physics, Southern University of Science and Technology, Shenzhen 518055, China
[8]Shenzhen Key Laboratory of Quantum Science and Engineering, Shenzhen 518055, China
[9]Central Research Institute, Huawei Technologies, Shenzhen 518129, China

(Received 27 May 2019; accepted 9 January 2020; published 3 February 2020)

We show that parity-time ($\mathcal{PT}$) symmetry can be spontaneously broken in the recently reported energy level attraction of magnons and cavity photons. In the $\mathcal{PT}$-broken phase, the magnon and photon form a high-fidelity Bell state with maximum entanglement. This entanglement is steady and robust against the perturbation of the environment, which is in contrast to the general wisdom that expects instability of the hybridized state when the symmetry is broken. This anomaly is further understood by the compete of non-Hermitian evolution and particle number conservation of the hybrid system. As a comparison, neither $\mathcal{PT}$-symmetry breaking nor steady magnon-photon entanglement is observed inside the normal level repulsion case. Our results may open an exciting window to utilize magnon-photon entanglement as a resource for quantum information science.

DOI: 10.1103/PhysRevLett.124.053602

Manipulating light-matter interaction is a long-lasting and intriguing topic for its pivotal role in quantum science and technologies. Recently, the strong coupling of magnons and cavity photons was intensively investigated with the aim of realizing quantum information transfer in hybrid spintronic systems [1–11]. Historically, the coherent magnon-photon coupling with a typical energy level repulsion (avoided crossing or anticrossing) spectrum was first identified by placing the magnetic insulator yttrium-iron-garnet (YIG) into a microwave cavity and (or) coplanar waveguide [1–8], whereas recent theory and experiments show that an abnormal anticrossing (energy level attraction) spectrum emerges by considering the feedback effect of photons [9–12]. Near the energy level repulsion, the magnon and photon hybridize to form an effective two-level platform, which launches a Rabi oscillation of the polariton and enables the coherent information transfer between magnons and photons [13]. However, the two energy levels of magnons and photons merge into a single band in the level attraction case, and it is not known how magnons and photons interplay to manifest their entanglement properties. This issue is urgent if one tends to bridge cavity spintronics with quantum information science, in which entanglement is an indispensable resource. Furthermore, the magnon-photon system with the feedback effect is not Hermitian any more, and there may exist complex eigenmodes [9–11]. This intriguing feature provides a generic platform to study non-Hermitian quantum physics and parity-time ($\mathcal{PT}$) symmetry [14,15].

In this Letter, we uncover the quantum correlation of magnons and photons inside the level attraction regime by solving their non-Hermitian dynamics, and we find that the magnon and photon form a maximally entangled Bell state in the $\mathcal{PT}$-broken phase. This emerging Bell state is steady, and thus not decaying with time, provided that (1) the decoherence can be well modelled by a Markovian process [16], and thus the widely used Lindblad formalism of noise applies [17]; and (2) the coupling strength of magnons and photons falls into the strong coupling regime, which has been realized in many experiments [2–7]. Compared with the traditional methods of generating Bell states [18–20], our proposal is of high fidelity, deterministic, and robust against dissipation. As we tune the magnon frequency, the system undergoes a phase transition to the $\mathcal{PT}$-exact phase, and the steady entanglement is replaced by an oscillating entanglement. Our results may open the door of non-Hermitian spintronics with $\mathcal{PT}$ symmetry, and they provide a new platform to use hybrid magnon polaritons as the entanglement resource.

 © 2020 American Physical Society

We consider a magnon-photon hybrid system with feedback action on the photons, which has been realized by coupling a magnet with various types of cavities [10–12,21]. The Hamiltonian of such a hybrid system can be written as

$$\mathcal{H} = \mathcal{H}_{\mathrm{FM}} + 1/2 \int (\epsilon_0 \mathbf{E}^2 + \mathbf{B}^2/\mu_0) dV - \sum_i \mathbf{S}_i \cdot \mathbf{h}_f, \quad (1)$$

where the first, second, and third terms are the ferromagnetic (FM), the electromagnetic (EM) wave, and the interaction parts of the Hamiltonian, respectively. $\mathcal{H}_{\mathrm{FM}}$ includes the exchange, anisotropy, and Zeeman energy. $\mathbf{E}$ and $\mathbf{B}$ are, respectively, the electric and magnetic components of the EM wave, with ϵ_0 and μ_0 being the vacuum permittivity and susceptibility, respectively. $\mathbf{S}_i$ is the spin of ith site, whereas the oscillating field $\mathbf{h}_f$ acting on the local spin includes a direct action of the microwave $\mathbf{h}_1 = \mathbf{h}e^{-i\omega_c t}$ and a reaction field of the precessing magnetization $\mathbf{h}_2 = \mathbf{h}_1 \delta e^{i\phi}$ [10,11], where ω_c is the microwave frequency; δ and ϕ are, respectively, the relative amplitude and phase of the two waves. In the low energy limit, we follow the standard quantization procedures of magnons and photons [22,23] and write the Hamiltonian as

$$\mathcal{H} = \omega_r a^\dagger a + \omega_c c^\dagger c + g(a^\dagger c + e^{i\Phi} a c^\dagger), \quad (2)$$

where a, c, $a^\dagger$, and $c^\dagger$ are annihilation and creation operators for magnons and photons, respectively [24,25]. ω_r is the magnon frequency, g is the effective coupling strength of magnons and photons, and $\tan\Phi/2 = -\delta \sin\phi/(1+\delta\cos\phi)$ is a tunable phase factor coming from the backaction effect. The effective Hamiltonian [Eq. (2)] can well describe the dissipative magnon-photon coupling in the experimental setup [10].

When $\Phi = k\pi (k = 0, 1, 2...)$, it is straightforward to show that the $\mathcal{PT}$ operation commutes with the Hamiltonian such that the system respects the $\mathcal{PT}$ symmetry. However, this does not guarantee that the $\mathcal{PT}$ operator and Hamiltonian display the same set of eigenstates due to the antilinearity of the $\mathcal{PT}$ operator [26,27]. If $\mathcal{PT}$ and $\mathcal{H}$ share simultaneous eigenstates with real eigenvalues, the phase is denoted as the $\mathcal{PT}$-exact phase. Otherwise, the phase is $\mathcal{PT}$ broken and characterized by complex eigenvalues [14]. Recently, the phase transition of $\mathcal{PT}$ symmetry was directly observed by placing two magnets inside a microwave cavity and adjusting the dissipation of the cavity [21].

To derive the spectrum, we perform a linear transformation of $a = \alpha\cos\theta + \beta e^{-i\Phi/2}\sin\theta$ and $c = -\alpha e^{i\Phi/2}\sin\theta + \beta\cos\theta$, where $\tan 2\theta = -2ge^{i\Phi/2}/(\omega_r - \omega_c)$; and we diagonalize the Hamiltonian [Eq. (2)] as $\mathcal{H} = \omega_1 \alpha^\dagger\alpha + \omega_2 \beta^\dagger\beta$, with the eigenvalues

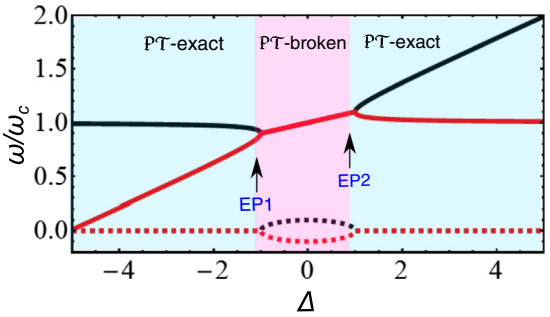

FIG. 1. Level attraction of the system described by Eq. (2) for $\Phi = \pi$. Detuning $\Delta \equiv (\omega_r - \omega_c)/2g$. Solid and dashed lines represent the real and imaginary parts of the eigenvalues, respectively. $g = 0.1\omega_c$.

$$\omega_{1,2} = \frac{1}{2}\left(\omega_r + \omega_c \pm 2g\sqrt{\Delta^2 + e^{i\Phi}}\right), \quad (3)$$

where $\Delta = (\omega_r - \omega_c)/(2g)$ is the detuning. Figure 1 shows a typical spectrum of level attraction ($\Phi = \pi$). Depending on whether the eigenvalues are real or not, two $\mathcal{PT}$-exact phases when $|\Delta| > 1$ and one $\mathcal{PT}$-broken phase when $|\Delta| < 1$, separated by two exceptional points at $|\Delta| = 1$ (EP1 and EP2), are identified. Next, we will show how the magnon and photon interplay to manifest their entanglement properties in these phases.

To proceed, it is essential to know how to describe the hybrid system within the framework of open quantum mechanics. In general, the state of the system can be represented by a biparty density matrix ρ. By recasting the effective Hamiltonian as the sum of a Hermitian operator $[\mathcal{H}_H \equiv (\mathcal{H} + \mathcal{H}^\dagger)/2]$ and an anti-Hermitian operator $[\mathcal{H}_A \equiv (\mathcal{H} - \mathcal{H}^\dagger)/2]$ (i.e., $\mathcal{H} = \mathcal{H}_H + \mathcal{H}_A$), the dynamic equation of the system can be expressed as [28]

$$\frac{\partial\rho}{\partial t} = -i[\mathcal{H}_H, \rho] - i\{\mathcal{H}_A, \rho\} + 2i\mathrm{tr}(\rho\mathcal{H}_A)\rho, \quad (4)$$

where the brackets [] and {} refer to the commutator and anticommutator, respectively. The third nonlinear term is added to preserve $\mathrm{tr}(\rho) = 1$.

To solve the evolution of density matrix governed by Eq. (4), we take an example of an initial pure state with a mean particle number of $N = \langle\mathcal{N}\rangle \equiv \langle a^\dagger a + c^\dagger c\rangle = 1$, whereas the general physics does not rely on this initial condition. One can immediately prove that $\partial N/\partial t = 0$ using the commutation relations $[\mathcal{N}, \mathcal{H}] = 0$. This implies that the particle number is conserved such that the Fock basis $\{|10\rangle, |01\rangle\}$ forms a complete set to describe the system. By solving the eigenequation $\mathcal{H}|\phi_k\rangle = \omega_k|\phi_k\rangle$, we can obtain the eigenstates as

$$|\phi_k\rangle = \cos\theta_k|10\rangle + e^{i\varphi_k}\sin\theta_k|01\rangle, \quad (5)$$

where θ_k and φ_k are determined by the relation $e^{i\varphi_k}\tan\theta_k = (\omega_k - \omega_r)/g$ $(k = 1, 2)$.

Suppose the initial state is

$$\rho_0 = |01\rangle\langle 01| = \sum_{k,j} p_{kj}|\phi_k\rangle\langle\phi_j|,$$

then the time-dependent density matrix can be formally written as [28]

$$\rho = \frac{e^{-i\mathcal{H}t}\rho_0 e^{i\mathcal{H}^\dagger t}}{\mathrm{tr}(e^{-i\mathcal{H}t}\rho_0 e^{i\mathcal{H}^\dagger t})} = \frac{\sum_{k,j} p_{kj} e^{-i\omega_{kj}t}|\phi_k\rangle\langle\phi_j|}{\sum_{k,j} p_{kj} e^{-i\omega_{kj}t}\mathrm{tr}(|\phi_k\rangle\langle\phi_j|)}, \tag{6}$$

where $\omega_{kj} = \omega_k - \omega_j^*$, and p_{kj} are the expansion coefficients. From this density matrix, the magnon-photon entanglement can be quantified through the logarithmic negativity defined as $E_N(\rho) = \ln||\rho^{T_c}||$, where ρ^{T_c} is the partial transpose of ρ with respect to mode c and $||\rho^{T_c}||$ refers to its trace norm [29]. Here, $E_N > 0$ is a sufficient and necessary condition for magnon-photon entanglement because the dimension of the Hilbert space $(2 \times 2 = 4)$ is not larger than six [30]. Next, we will present the results for the energy level attraction and repulsion cases, respectively.

For the level attraction case of $\Phi = \pi$, according to the magnitude of detuning shown in Fig. 1, three regimes can be classified.

$\mathcal{PT}$-broken phase when $|\Delta| < 1$.—Here, both ω_1 and ω_2 are complex numbers, and we can derive $\omega_{12} = \omega_{21} = 0$, $\omega_{11} = -\omega_{22} = 2ig\sqrt{1-\Delta^2}$, and the expansion coefficients $p_{11} = p_{22} = -p_{12} = -p_{21} = (1-\Delta^2)^{-1}/2$. As $t \to \infty$, the ω_{11} term dominates both the numerator and denominator of Eq. (6) such that the steady density matrix $\rho(t \to \infty) = |\phi_1\rangle\langle\phi_1|$. Here, $|\phi_1\rangle = (|10\rangle + e^{i\varphi_1}|01\rangle)/\sqrt{2}$, where $\varphi_1 = \arccos\Delta$ with the entanglement $E_N(|\phi_1\rangle\langle\phi_1|) = \ln 2$. Note that this is a maximally entangled state for the biparty (each with two-dimensional Hilbert space) and is the same as the Bell state, except for the controllable global phase $e^{i\varphi_1}$. Figure 2(a) shows the time evolution of the magnon-photon entanglement (red dashed line) by numerically solving Eq. (4), which is consistent with the prediction. To measure the distance between the intermediate state and the steady Bell state, we have introduced the fidelity of the Bell state defined as $F(|\phi_1\rangle, \rho) = \mathrm{tr}\sqrt{\langle\phi_1|\rho|\phi_1\rangle}$ [31]. Clearly, F approaches one as the system evolves to the Bell state $|\phi_1\rangle$. Figure 2(b) shows the entanglement and fidelity of the steady state as a function of the purity of the initial states, where the initial state is pure if its purity is equal to one, whereas it is mixed if the purity is located in the range of [0.5,1). The constant trend in Fig. 2(b) indicates that the generation of the steady Bell state does not rely on the nature of the initial states. It can be understood as follows: The non-Hermitian nature of the $\mathcal{PT}$-symmetric Hamiltonian results in two eigenmodes with a generic gain (ω_1 mode with positive imaginary component) and loss (ω_2 mode with negative imaginary component) in the broken phase. The particle number in the gain mode will keep increasing until all the particles are pumped into this state; i.e., the system behaves as an attractor. Mathematically, inclusion of the nonlinear term in Eq. (4) is a typical treatment to effectively model the non-Hermitian system. It can be justified by putting the system of interest into a larger Hermitian system, as well as by further tracing the irrelevant information as the environment. This is important to get a steady dynamics of the system, and its correctness is justified by comparing the normalized population with the experiments [32].

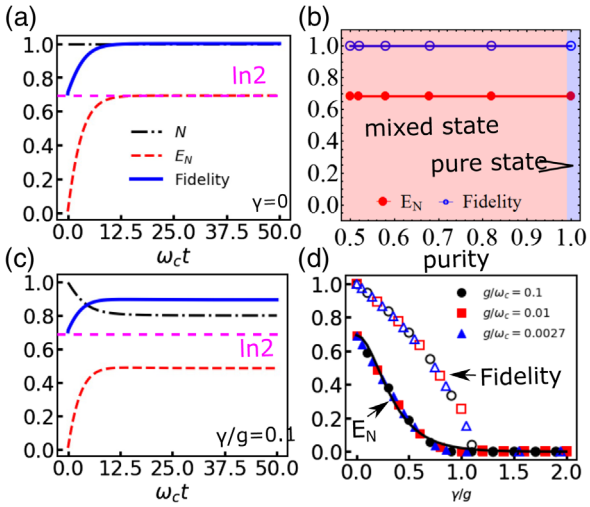

FIG. 2. (a) Time evolution of particle number N and entanglement measure E_N under resonance: $g = 0.1\omega_c$ and $\rho_0 = |01\rangle\langle 01|$. (b) Steady entanglement and fidelity of final state with respect to Bell state as a function of purity of the initial state: $\rho_0 = p|01\rangle\langle 01| + (1-p)|10\rangle\langle 10|$. When $p = 1$, ρ_0 is a pure state with purity equal to one, whereas it gives a mixed state with purity in range [0.5, 1) when $0 < p < 1$. Figure 2(c) is similar to 2(a), but with dissipation of $\gamma = 0.1g$. The dashed pink line indicates the magnon-photon entanglement without dissipation. For simplicity, we choose $\gamma_1 = \gamma_2 = \gamma$ in the calculations. (d) Magnon-photon entanglement and fidelity of the steady state as functions of dissipation: $\Delta = 0$.

To verify the robustness of this steady Bell state against the environment, we introduce dissipation by adding standard Lindblad operator [17]

$$\mathcal{L}\rho = \sum_i \gamma_i(2\xi_i^\dagger\rho\xi_i - \xi_i^\dagger\xi_i\rho - \rho\xi_i^\dagger\xi_i)$$

into Eq. (4), where $\xi_{1,2} = a$ and c, and γ_1 and γ_2 are the damping of the magnon and photon, respectively. By solving the dynamic equation, we obtain the time dependence of the magnon-photon entanglement as well as the fidelity in Fig. 2(c). Now, the steady state is close but not equal to the Bell state $(F < 1)$, whereas the steady entanglement is smaller than the system without dissipation (dashed pink line). This is expected because the interaction

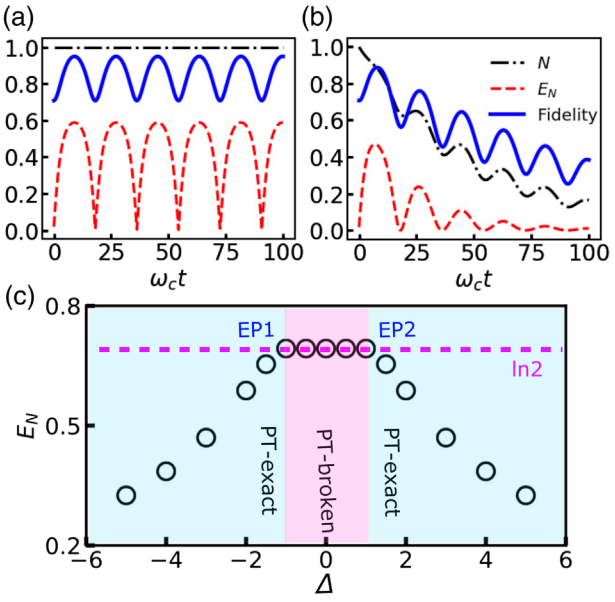

FIG. 3. Time evolutions of particle number N and entanglement measure E_N away from resonance for $\gamma = 0$ (a) and $\gamma = 0.1g$ (b), respectively: $g = 0.1\omega_c$ and $\Delta = 2$. (c) Full phase diagram of the system with a $\mathcal{PT}$-broken phase sandwiched by two $\mathcal{PT}$-exact phases. Data in the $\mathcal{PT}$-exact phase are taken as maximum magnon-photon entanglement during Rabi oscillation.

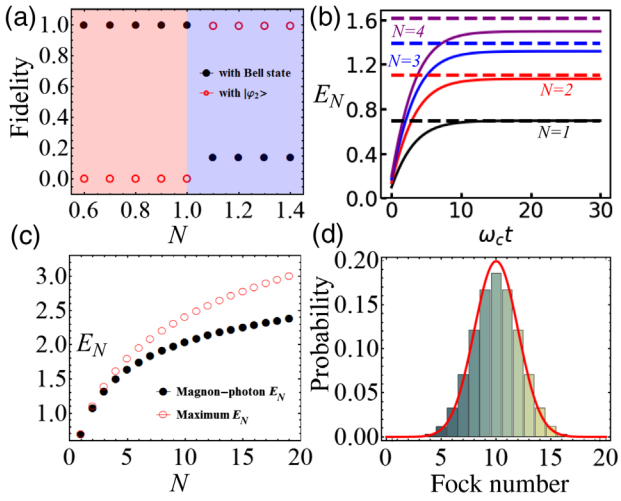

FIG. 4. (a) Influence of imperfect photon source on fidelity of maximally entangled state. (b) Time evolutions of magnon-photon entanglement for $N = 1$ (black line), 2 (red line), 3 (blue line), and 4 (purple line), respectively. Horizontal dashed lines represent maximal entanglement. (c) Steady magnon-photon entanglement as a function of total excitation number (black dots) in $\mathcal{PT}$-broken phase. Red circles represent maximum biparty entanglement of $E_N = \ln(N+1)$: $\Delta = 0$. (d) Probability distribution of Fock number of magnons when $N = 19$. Red line is a Gaussian distribution. $\gamma = 0.01g = 0.001\omega_c$.

of a quantum system with the environment usually induces the decay of entanglement, with only a few exceptions [33,34]. Figure 2(d) shows the entanglement as a function of dissipation at various coupling strengths g. Interestingly, the curves with different g perfectly scale in one curve with a critical point at $\gamma/g = 1$; beyond which, the entanglement of the steady state disappears. We estimate the fidelity of our Bell state to be 97.85% using realistic experimental parameters by placing a millimeter-sized YIG sphere inside a Fabry-Perot cavity and measuring the input or output fields ($g/\omega_c = 0.0027$, $\gamma_a = 7.6 \times 10^{-5}$, and $\gamma_c = 1.5 \times 10^{-4}$ [10]).

$\mathcal{PT}$-exact phase when $|\Delta| > 1$.—Here, both $\omega_{1,2}$ and ω_{ij} are real; hence, the elements of the density matrix as well as the resulting magnon-photon entanglement will keep oscillating with time, as shown in Fig. 3(a). No steady state is found. Once the spontaneous decay of the magnon-photon mode is considered, the particle number of the system will decay toward zero exponentially, and it will be accompanied by the oscillating decay of the magnon-photon entanglement toward zero, as shown in Fig. 3(b). Note that the magnon-photon couplings are beam-splitter-types in both the $\mathcal{PT}$-exact and -broken phases, whereas their steady properties are different. This suggests that the symmetry property of the Hamiltonian matters instead of the coupling type.

Exceptional points at $|\Delta| = 1$.—The system has degenerate eigenvalues [35] $(\omega_1 = \omega_2 = (\omega_r + \omega_c)/2)$ and eigenvectors $(|\phi_1\rangle = |\phi_2\rangle = (|10\rangle \pm |01\rangle)/\sqrt{2})$. It will gradually decay into a state with zero entanglement due to dissipation.

A full phase diagram of the system is plotted in Fig. 3(c). In the $\mathcal{PT}$-broken phase, the magnon-photon entanglement is always steady and maximal ($\ln 2$), regardless of the magnitude of detuning. In the $\mathcal{PT}$-exact phase, the magnon-photon performs a Rabi oscillation, and thus their entanglement oscillates. The maximum entanglement decreases monotonically as the detuning increases, which suggests that the steady state is more close to a separable state at large detuning.

For the level repulsion case of $\Phi = 0$, the Hamiltonian is Hermitian with real eigenvalues such that it is also $\mathcal{PT}$ exact. The resulting magnon-photon entanglement will keep oscillating with time, and no steady entanglement exists, which is similar to the $\mathcal{PT}$-exact regime of the level attraction.

We concentrated our previous effort in the Hilbert subspace of $N = 1$. If this is not true due to the influence of temperature and the imperfection of the photon source, the total particle number of initial states will not be equal to one exactly. To address this issue, we consider a fluctuation of the particle number around one and show the fidelity of the steady state with respect to the Bell state as a function of the particle number in Fig. 4(a). Given $N \leq 1$, the steady state is always a high-fidelity Bell state, whereas it deviates from the Bell state severely for $N > 1$. Interestingly, the steady state at $1 < N < 2$ becomes a maximally entangled bi-qutrit: $|\varphi_2\rangle = 1/\sqrt{3}(|02\rangle + |11\rangle + |20\rangle)$.

Generally, the maximally entangled N-particle state reads

$$|\varphi\rangle = 1/\sqrt{N+1}\sum_{k=0}^{N}|k, N-k\rangle$$

with logarithmic negativity $E_N = \ln(N+1)$, where k and $N-k$ refer to the occupations of magnons and photons, respectively. Figure 4(b) shows that the steady entanglement is close to this maximal entanglement (horizontal dashed lines) for $N = 2$, 3, and 4, respectively [36]. As N increases further, the steady state has larger entanglement, but it deviates more from the maximally entangled state, as shown in Fig. 4(c). When the number of particles becomes considerably large, the steady state is a Gaussian state, as illustrated in Fig. 4(d) with $N = 19$. This may be useful if one intends to produce an N-particle Gaussian state. Nevertheless, if one tends to generate a Bell state, the average particle number needs to be less than one. This means that the cryogenic environment is essential to generate a Bell state. For the commonly used material YIG, the lowest lying magnon energy is 101 mK [37]; then, the typical temperature to excite only one magnon mode can be estimated from a Bose-Einstein distribution as 146 mK, which is accessible in experiments. Alternatively, one may use a photon source with an average photon number smaller than one [38].

Furthermore, the entanglement among the magnon, photon, and phonon can also be created through the nonlinear Kerr effect or magnetostrictive interaction [39–41]; however, the generated entanglement is around 0.2, which is much smaller than our finding, and this is probably because of the smallness of the nonlinear effect.

In conclusion, we have studied the entanglement properties of magnons and photons inside a cavity and found that the magnon-photon can form a Bell pair with maximum entanglement in the $\mathcal{PT}$-broken phase of the system, whereas no steady entanglement is identified in the $\mathcal{PT}$-exact phase. The generated Bell pair is of high fidelity and robustness against dissipation, and it is insensitive to the small detuning between the magnon frequency and photon frequency. To detect the magnon-photon entanglement, one can measure the particle number fluctuation of the system or perform tomography on the density matrix [42,43]. The generation of the magnon-photon Bell pair provides an alternate to achieve a maximally entangled state in the solid state system, and it may be utilized as a resource for quantum tasks, such as quantum sensing and channel discrimination [44,45].

We acknowledge G. E. W. Bauer, Ka Shen, and V. L. Grigoryan for helpful discussions. H. Y. Y. acknowledges the financial support from the National Natural Science Foundation of China (NSFC) (Grant No. 61704071) and the Shenzhen Fundamental Subject Research Program (No. JCYJ20180302174248595). P. Y. was supported by NSFC (Grants No. 11604041 and No. 11704060) and the National Key Research Development Program under Contract No. 2016YFA0300801. Q. Y. H. acknowledges the NSFC (Grants No. 11622428, No. 61675007, and No. 11975026) and the Beijing Natural Science Foundation (Z190005). K. X. acknowledges the support of NSFC (Grant No. 11734004) and NSAF (Grant No. U1930402). M.-H. Y. acknowledges the Natural Science Foundation of Guangdong Province (Grant No. 2017B030308003), the Key Research and Development Program of Guangdong Province (Grant No. 2018B030326001), the Guangdong Innovative and Entrepreneurial Research Team Program (Grant No. 2016ZT06D348), the Science, Technology and Innovation Commission of Shenzhen Municipality (Grants No. JCYJ20170412152620376 and No. JCYJ20170817105046702 and No. KYTDPT20181011104202253), NSFC (Grants No. 11875160 and No. U1801661), the Economy, Trade and Information Commission of Shenzhen Municipality (Grant No. 201901161512).

*huaiyangyuan@gmail.com
†yung@sustech.edu.cn

[1] Ö. O. Soykal and M. E. Flatté, Phys. Rev. Lett. **104**, 077202 (2010).
[2] H. Huebl, C. W. Zollitsch, J. Lotze, F. Hocke, M. Greifenstein, A. Marx, R. Gross, and S. T. B. Goennenwein, Phys. Rev. Lett. **111**, 127003 (2013).
[3] Y. Tabuchi, S. Ishino, T. Ishikawa, R. Yamazaki, K. Usami, and Y. Nakamura, Phys. Rev. Lett. **113**, 083603 (2014).
[4] X. Zhang, C.-L. Zou, L. Jiang, and H. X. Tang, Phys. Rev. Lett. **113**, 156401 (2014).
[5] M. Goryachev, W. G. Farr, D. L. Creedon, Y. Fan, M. Kostylev, and M. E. Tobar, Phys. Rev. Applied **2**, 054002 (2014).
[6] L. Bai, M. Harder, Y. P. Chen, X. Fan, J. Q. Xiao, and C.-M. Hu, Phys. Rev. Lett. **114**, 227201 (2015).
[7] Y.-P. Wang, G.-Q. Zhang, D. Zhang, T.-F. Li, C.-M. Hu, and J. Q. You, Phys. Rev. Lett. **120**, 057202 (2018).
[8] Y. Cao, P. Yan, H. Huebl, S. T. B. Goennenwein, and G. E. W. Bauer, Phys. Rev. B **91**, 094423 (2015).
[9] V. L. Grigoryan, K. Shen, and K. Xia, Phys. Rev. B **98**, 024406 (2018).
[10] M. Harder, Y. Yang, B. M. Yao, C. H. Yu, J. W. Rao, Y. S. Gui, R. L. Stamps, and C.-M. Hu, Phys. Rev. Lett. **121**, 137203 (2018); Y. Yang, J. W. Rao, Y. S. Gui, B. M. Yao, W. Lu, and C.-M. Hu, Phys. Rev. Applied **11**, 054023 (2019); P.-C. Xu, J. W. Rao, Y. S. Gui, X. Jin, and C.-M. Hu, Phys. Rev. B **100**, 094415 (2019).
[11] B. Bhoi, B. Kim, S.-H. Jang, J. Kim, J. Yang, Y.-J. Cho, and S.-K. Kim, Phys. Rev. B **99**, 134426 (2019).
[12] I. Boventer, C. Dorfinger, T. Wolz, R. Macêdo, R. Lebrun, M. Kläui, and M. Weides, arXiv:1904.00393.

[13] Y. Tabuchi, S. Ishino, A. Noguchi, T. Ishikawa, R. Yamazaki, K. Usami, and Y. Nakamura, Science **349**, 405 (2015).
[14] R. El-Gananiny, K. G. Makris, M. Khajavikhan, Z. H. Musslimani, S. Rotter, and D. N. Christodoulides, Nat. Phys. **14**, 11 (2018).
[15] Y. Cao and P. Yan, Phys. Rev. B **99**, 214415 (2019).
[16] The Markovian approximation means that the spin relaxation time due to its interaction with the environment is much longer than the bath relaxation time such that the memory effect can be ignored. This is well justified in a magnet system because the spin relaxation is typically in the gigahertz regime, whereas the relaxation through phonons is in the regime of tens of terahertz.
[17] G. Lindblad, Commun. Math. Phys. **48**, 119 (1976).
[18] P. G. Kwiat, K. Mattle, H. Weinfurter, A. Zeilinger, A. V. Sergienko, and Y. Shih, Phys. Rev. Lett. **75**, 4337 (1995).
[19] A. Kowalewska-Kudlaszyk, W. Leoński, and J. Peřina, Jr., Phys. Scr. **T147**, 014016 (2012).
[20] D. Shwa, R. D. Cohen, A. Retzker, and N. Katz, Phys. Rev. A **88**, 063844 (2013).
[21] J. Zhao, Y. Liu, L. Wu, C.-K, Duan, Y.-x. Liu, and J. Du, arXiv:1908.03358v1.
[22] H. Y. Yuan and X. R. Wang, Appl. Phys. Lett. **110**, 082403 (2017).
[23] H. Y. Yuan, S. Zheng, Z. Ficek, Q. Y. He, and M.-H. Yung, Phys. Rev. B **101**, 014419 (2020).
[24] Here, a and $a^{\dagger}$ are the quantizations of the uniform precession mode, i.e., the Kittel mode. The higher energy magnon modes are safely neglected because the photon moves much faster than magnon, and then they only couple in the limit of zero wave vector (i.e., the Kittel mode) to match the frequency.
[25] The non-Hermitian nature is crucial to determine the steady entanglement of modes a and b. In most of the traditional systems with beam-splitter-type interaction, such as cavity optomechanics and the interacting system of distinguishable particles, the Hamiltonian is Hermitian and they cannot give any finite steady entanglement, as discussed in the level repulsion case of the current work. In principle, if one could have the non-Hermitian coupling as we studied here, the steady entanglement presented here could be directly applied.
[26] C. M. Bender and S. Boettcher, Phys. Rev. Lett. **80**, 5243 (1998).
[27] J. Schindler, A. Li, M. C. Zheng, F. M. Ellis, and T. Kottos, Phys. Rev. A **84**, 040101(R) (2011).
[28] D. C. Brody and E.-M. Graefe, Phys. Rev. Lett. **109**, 230405 (2012).
[29] G. Vidal and R. F. Werner, Phys. Rev. A **65**, 032314 (2002).
[30] M. Horodecki, P. Horodecki, and R. Horodecki, Phys. Lett. A **223**, 1 (1996).
[31] M. A. Nielsen and I. L. Chuang, *Quantum Computation and Quantum Information*, 10th ed. (Cambridge University Press, Cambridge, England, 2010).
[32] Y. Wu, W. Liu, J. Geng, X. Song, X. Ye, C.-K. Duan, and X. Rong, and J. Du, Science **364**, 878 (2019).
[33] H. Y. Yuan and M.-H. Yung, Phys. Rev. A **98**, 022125 (2018).
[34] H. Y. Yuan and M.-H. Yung, Phys. Rev. B **97**, 060405(R) (2018).
[35] M. Ali-Miri and A. Alù, Science **363**, eaar7709 (2019).
[36] Here, we have compared the entanglement of quantum states measured by log negativity and von Neumann entropy, and we find that they give consistent results, which suggest that logarithmic negativity is still a good measure in our consideration.
[37] S. O. Demokritov, V. E. Demidov, O. Dzyapko, G. A. Melkov, A. A. Serga, B. Hillebrands, and A. N. Slavin, Nature (London) **443**, 430 (2006).
[38] J. G. Bohnet, Z. Chen, J. M. Weiner, D. Meiser, M. J. Holland, and J. K. Thompson, Nature (London) **484**, 78 (2012).
[39] J. Li, S.-Y. Zhu, and G. S. Agarwal, Phys. Rev. Lett. **121**, 203601 (2018).
[40] J. Li and S.-Y. Zhu, New J. Phys. **21**, 085001 (2019).
[41] Z. Zhang, M. O. Scully, and G. S. Agarwal, Phys. Rev. Research **1**, 023021 (2019).
[42] W. P. Bowen, R. Schnabel, P. K. Lam, and T. C. Ralph, Phys. Rev. Lett. **90**, 043601 (2003).
[43] A. Orieux, A. Eckstein, A. Lemaître, P. Filloux, I. Favero, G. Leo, T. Coudreau, A. Keller, P. Milman, and S. Ducci, Phys. Rev. Lett. **110**, 160502 (2013).
[44] D. Lachance-Quirion, Y. Tabuchi, S. Ishino, A. Noguchi, T. Ishikawa, R. Yamazaki, and Y. Nakamura, Sci. Adv. **3**, e1603150 (2017).
[45] M. Piani and J. Watrous, Phys. Rev. Lett. **102**, 250501 (2009).